Residual dipolar couplings as a tool for structural analysis of ionic liquids†

Higor D. F. de Melo, [a] Daiane S. Carvalho, [a] Fernando Hallwass, [a] Ulrich Sternberg [bc] and Armando Navarro-Vázquez *[a]

An acrylonitrile/dimethylacrylamide cross-linked polymer could be swollen in different imidazolium ionic liquids. Mechanical compression of the obtained polymer gels inside an NMR tube allowed the measurement of residual dipolar couplings. Conformational analysis of the 1-methyl-3-butyl-imidazolium (BMIM) cation could be performed by including the measured RDCs as restraints in time-averaged molecular dynamics.

Mechanically strained polymer gels, swollen in a variety of deuterated solvents, allow easy measurement of residual dipolar couplings (RDCs) that can be applied then to structural elucidation purposes in organic molecules.[1–4] Among them, those which allow reversible mechanical compression, present several advantages such as short swelling and equilibration times, and easy sample recovery.[5] Following on from the original PMMA/$CDCl_3$ system, other combinations of polymers/solvents have been reported such as poly-DEGMEMA/CD_3OD,[6] poly-HEMA/DMSO-d_6,[7] and polyacrylonitrile (PAN)/DMSO-d_6[8] and even water compatible systems.[9,10]

Ionic liquids (ILs) are a large and important family of solvents. They are room temperature molten organic salts, very often composed of an organic cation and an inorganic counterion. A very comprehensive literature exist on their structure and properties, including NMR studies.[11–13] Homo (NOESY/ROESY) and heteronuclear (HOESY) NOE based experiments have been used to probe cation-cation and cation-anion interaction in ILs, as well as intermolecular interactions with solutes such as CO_2.[14,15]

In 2013 Dama and Berger showed that RDC values of carbohydrates could be extracted in lyotropic nematic ionic liquids self-oriented in the presence of a magnetic field.[16] However, to the best of our knowledge, no attempt has been done to structurally analyse ionic liquids using RDCs. We will show here that polymer gels can be swollen in ionic liquids and mechanically compressed to provide RDCs that can then be applied to the conformational analysis of the IL organic cation.

We began our study trying to swell ionic liquids, of the imidazolium family (Table 1) in cross-linked polymers with different degrees of polarity, namely polydimethylsiloxane (PDMS),[17] polystyrene,[18] poly-HEMA,[7] and PAN.[8] These two later acrylate gels were prepared in our laboratory following the published procedures, whereas PDMS and polystyrene gel were generously provided to us. In these single monomer gels no noticeable swelling could be observed for any of the tested ILs, however, a copolymer consisting of a 75 : 25 v/v mixture of *N*,*N*-dimethylacrylamide (DMA) and acrylonitrile (AN) cross-linked with a 0.5 mol% of ethylene glycol diacrylate (EGDA) allowed to observe appreciable swelling on imidazolium based ILs such as BMIM•NTf_2^-, BMIM and EMIM•BF_4^-, and BMIM•$[N(CN)_2]^-$ (Table 1).

After observation of this swelling behaviour, we cut three pieces, 2.5 cm long, of the p-DMA/AN copolymer and let it swell in BMIM•NTf_2^-, BMIN and EMIM•BF_4^- and BMIM•$[N(CN)_2]^-$. Note that swelling in BMIM•BF_4^- required a much longer time, nearly three weeks, than for the other ILs which were completely swollen in 5–7 days. For this practical reason RDCs were not recorded for BMIM•BF_4^- IL. Compression of the gel allowed the measurement of the $^1D_{CH}$ RDCs, for the imidazolium cations, by

Table 1 Swelling tests for different polymer/IL combinations

Polymer gel	Swelling				
	i	**ii**	**iii**	**iv**	**v**
PDMA	No	No	No	—	—
PAN	No	No	No	No	—
poly-HEMA	No	No	No	No	—
Polystyrene	No	No	No	No	—
PDMS	No	No	No	No	—
p-DMA/AN	Yes	Yes	No	Yes	Yes

i) BMIM•BF_4^- **ii)** BMIM•NTf_2^- **iii)** BMIM•PF_6^- **iv)** EMIM•BF_4^- **v)** BMIM•$[N(CN)_2]^-$

[a] *Departamento de Química Fundamental, Centro de Ciências Exatas e da Natureza (CCEN), Universidade Federal de Pernambuco, Avenida Jornalista Fernandes s/n. Cidade Universitária, Recife, Pernambuco 50740-560, Brazil*

[b] *Research Partner of Karlsruhe Institute of Technology (KIT), Karslruhe, Germany*

[c] *COSMOS-Software, Jena, Germany. Web: https://www.cosmos-software.de*

† Electronic supplementary information (ESI) available. See DOI: https://doi.org/10.1039/d3cc00929g

Table 2 $^{1}D_{CH}$ RDC values of BMIM and EMIM cations in the BMIM•NTf_2^-, EMIM•BF_4^-, and BMIM•$[N(CN)_2]^-$

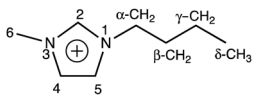

BMIM

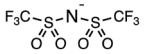

NTF_2^-

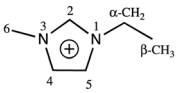

EMIM

BF_4^-

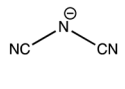

$[N(CN)_2]^-$

	$^{1}D_{CH}$ (Hz)		
Site	BMIM•NTf_2^-	EMIM•BF_4^-	BMIM•$[N(CN)_2]^-$
δ-$\underline{C}H_3$	−0.1	—	0.1
γ-$\underline{C}H_2$	−0.8	—	−1.4
β-$\underline{C}H_2$	−3.8	0.5	−1.6
α-$\underline{C}H_2$	−8.2	−2.2	−3.8
6	−3.8	−2.0	−2.5
5	−1.1	0.3	0.9
4	5.3	2.9	2.9
2	−10.7	−0.6	−3.7

just measuring two $\{^{1}H\}$-^{13}C gated decoupled experiments[19] in the relaxed and compressed states of the gel. The RDCs were then determined as the difference $^{1}D_{CH} = {}^{1}T_{CH} - {}^{1}J_{CH}$ between the one-bond proton-carbon couplings in the compressed ($^{1}T_{CH}$) and relaxed states of the gel ($^{1}J_{CH}$). RDC values for the imidazolium cation, in the different ionic liquids, are presented in Table 2. The RDC values are small probably due to the small size of the BMIM and EMIM cations. The larger RDCs were obtained for the BMIM•NTf_2^- IL and this set of values was, therefore, chosen for application to the conformational analysis of the BMIM cation since it should, a priori, provide a more accurate result.

The conformational analysis of the BMIM cation was started by exploring its conformational space using a Monte Carlo based procedure, as implemented in the GMMX[20] program, using the MMFF94[21] force field. The geometry of each conformation was then refined at the DFT M062X/6-31+G** level *in vacuo*.[22]

All BMIM conformations possessing C_1 symmetry must be present in the achiral polymer-gel/IL medium as an equally populated enantiomeric pair. By choosing a particular sign for the torsion around the N1-CH2α bond, diastereoisomeric conformations arise from rotation around the CH_2α-CH2β and CH_2β-CH2γ bonds. Each of these rotations produces three limiting conformations, (+)-*gauche* (G+), (−)-*gauche* (G−), and *anti* (A). accounting for nine possible diastereoisomeric conformations, as actually found by the GMMX program (Fig. 1).

A previous conformational analysis of BMIM in the BMIM•BF_4^- IL was based on the use of IR/Raman vibrational spectroscopies in combination with *ab initio* calculations.[23] The authors considered only four conformation namely, GA, AA, AG, and GG, (Fig. 1), since the relative disposition respect to the imidazolium cation was not considered. They estimated, from

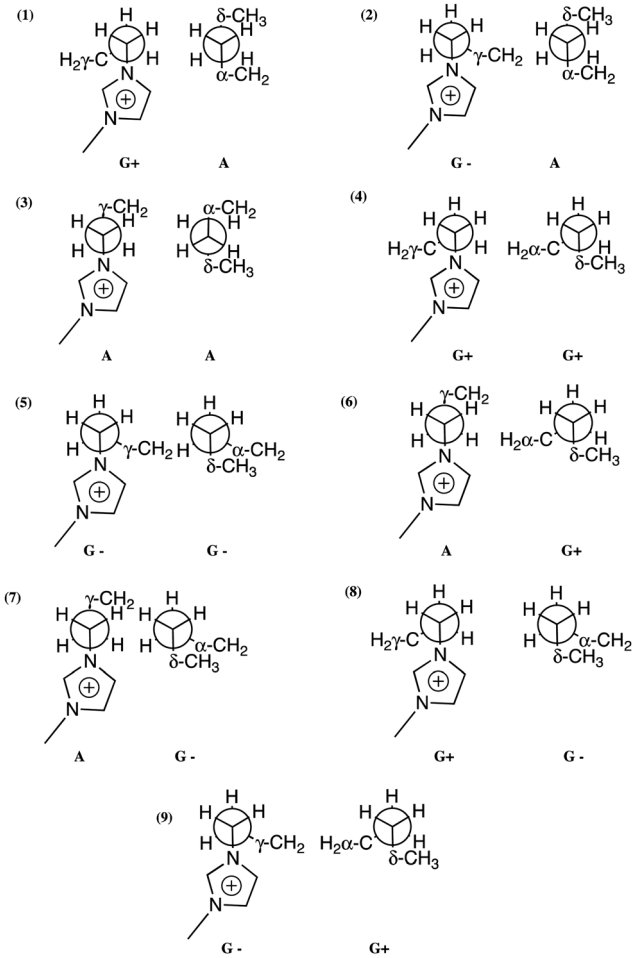

Fig. 1 Newman projections of the different conformational states of the BMIM cation.

analysis of the spectral data, populational weights of 0.48, 0.28, 0.17, and 0.07, respectively.

Singular value decomposition of the experimental RDCs, using the MSpin package,[24] on the individual DFT geometries provided a best fit (quality factor, Q = 0.136)[25] for the G+ G+ conformation (Table 3). However, at the light of the *in vacuo* DFT energy differences (Table 3), the observed $^{3}J_{HH}$ coupling patterns of the side chain in the ^{1}H NMR spectrum (Fig. S1, ESI†), as well

Table 3 Computed DFT energies, derived Boltzmann populations and individual RDC quality factors for BMIM conformations

Conformation	ΔE^a	Pop^b (%)	Q^c
G+ A	0.00	28.9	0.217
G− A	0.47	13.0	0.204
A A	0.70	8.9	0.199
G+ G+	0.14	22.8	0.136
G− G−	0.64	9.8	0.293
A G+	1.11	4.4	0.234
A G−	1.08	4.7	0.303
G+ G−	1.02	5.1	0.213

[a] Relative SCF energies in kcal mol^{-1}. [b] Boltzmann populations at 298.15 K. [c] Quality factor.

as the previous IR analysis,[23] it is clear that BMIM should have several largely populated conformations in solution. Since, for such an small molecule like BMIM, conformational jumping in the side chain greatly changes the overall molecular shape, the single alignment tensor approximation,[26] where equal resampling of rotational states respect to an unique coordinate frame is assumed for all conformations, can easily break. In fact, when trying to fit populations in two-membered ensembles, a best solution with $Q = 0.083$ is found for a 93 : 7 combination of G+ G+ and G− G− conformations. Although the conformationally-averaged back-predicted RDCs fit very well the observed ones, predicted RDCs for the G− G− conformations are nearly one order of magnitude larger than those predicted for G+ G+ indicating that application of the single tensor approximation for the BMIM system is meaningless (See ESI†).

Therefore, we decided to apply the Molecular Dynamics with Orientational Constraints (MDOC) approach to this particular problem,[27] a molecular dynamics (MD) method based on the use of per-coupling dipolar coupling tensors rather than a molecular alignment tensor, where experimental RDC tensors are introduced as time-averaged restraints into a molecular dynamics-run. Dipolar coupling tensors and their gradients are computed at each step of the MD run. The pseudo-forces obtained in this way power molecular rotations that induce the necessary conformational jumps to fit the conformationally-averaged experimental RDCs. It should be emphasized that there is a principal difference between the methods that work with a set of fixed pre-calculated structures and MDOC since the latter generates a sequence of structures that resembles the distribution of conformers at ambient temperatures, in this case at 303.4 K. The MDOC obtained conformational distributions reflect Gibbs free energy differences including the entropic term $-T\Delta S$ rather than energy differences.[28] Flat broad energy valley, as the ones arising here from sp^3–sp^3 and sp^3–sp^2 bond rotations, can allow for a multitude of structures leading to a larger entropy term and may be preferred over a sharp deep energy cusp. We named this dipolar coupling driver simulation as $MDOC_D$.

In a second simulation on the BMIM cation ($MDOC_{D,J}$), additionally to the RDC constraints $^3J_{HH}$ couplings between Hα, Hβ and Hγ protons are used as additional constraints which help to better define the conformational distribution of the butyl side-chain. Again, the analysis was done using BMIM•NTf_2^- experimental values. All calculated RDCs in the $MDOC_D$ and $MDOC_{D,J}$ runs were in accordance with the experimental values within the estimated experimental error bounds of 0.5 Hz (see ESI†). The $MDOC_{D,J}$ simulation should produce more trustful results since it fulfils, additionally to the fifteen RDC constraints, four independent $^3J_{HH}$ constraints.‡

Analysis of the MD run provides a rather flat distribution (Fig. 2), as *a priori* expected from the small energy differences between BMIM conformations (Table 3). The C2-N1-Cα-Cβ torsion profile (upper pane of Fig. 2) indicates a slight preference for the Cα–Cβ bond pointing perpendicularly to the imidazolium ring plane which agrees with the optimized DFT geometries. The summed $MDOC_{D,J}$ populations for the GG, GA, AG and AA conformational families amount to 30, 26, 28, and 16% respectively (Table 4). The overall results point to a flatter distribution than that obtained by Holomb. The introduction of the $^3J_{HH}$ restraints leads to a significant suppression of the G− type conformers of the Cα–Cβ bond and to a smaller extent the G− conformers of the Cβ–Cγ bond (see also ESI†).

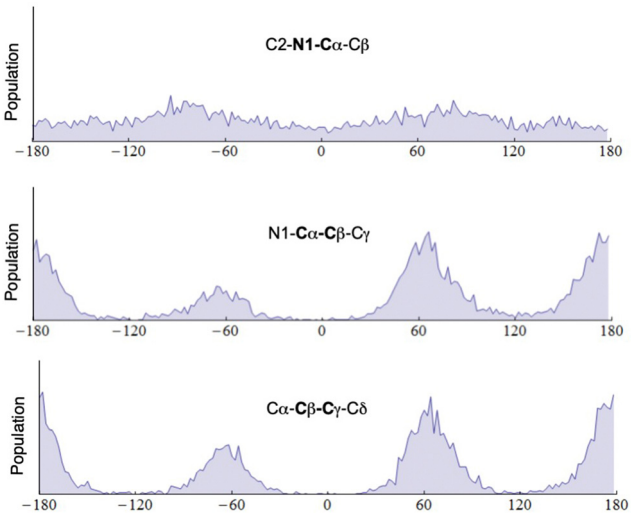

Fig. 2 Torsion profiles for the BMIM cation from the time-averaged RDC and $^3J_{HH}$ $MDOC_{D,J}$ run.

Table 4 $MDOC_D$ and $MDOC_{D,J}$ derived conformational populations for the BMIM cation

	Population (%)			
Conformation	IR/Raman[a]	$MDOC_D$[b]	$MDOC_{D,J}$[c]	DFT[d]
G+ A; G− A	— [48][e]	15; 15 [30]	18; 8 [26]	42
A A	28	10	16	10
A G+; A G−	— [17]	13; 14 [27]	18; 10 [28]	9
G+ G+; G− G−	7	10;11 [21]	15; 4 [19]	33
G+ G−; G− G+	—[e]	6; 6 [12]	7; 4 [11]	8

[a] From ref. 23. [b] RDC only MDOC run. [c] RDC+ $^3J_{HH}$ MDOC run. [d] This work DFT derived Boltzmann populations. [e] Sum of G+ and G− forms in brackets; G+ and G− forms were not differentiated in ref. 23.

The obtained RDCs can be used to solve not only conformational but also configurational and assignment problems. As an example, we could verify the assignment of BMIM protons H4 and H5 by adjusting only the $^1D_{CH}$ data corresponding to the imidazolium ring. That is, the $^1D_{CH}$ RDCs corresponding to positions 2, 4 and 5 of the imidazolium ring as well as the *N*-methyl group. To accomplish that, an SVD adjustment was performed taking only into account the *Axx*, *Axy* and *Axz* elements of the alignment tensor. The assignment corresponding to H4 being the most shielded proton corresponded to a quality factor of 0.058 while a value of 0.144 is obtained for the inverse assignment. This was in perfect agreement with observations from 1D-NOESY experiments[29] (See ESI†). Noteworthy, the rotational correlation time of the BMIM cation largely increases inside the swollen polymer-gel since the sign

of NOE in the BMIM cation switch from positive to negative in going from the isotropic layer surrounding the gel to the IL inside the gel (Fig. S6, ESI†).

In summary, the use of RDCs obtained by using polymer gels as weakly aligning media of ionic liquids allows to obtain quantitative information about conformational state of the IL organic cation as well as to solve configurational/assignment problems. We expect that the present work will open a new way for the NMR structural analysis of ILs, particularly, considering that polymer/IL combinations may form ionogel conductive composite materials with important applications in electronic devices. In this regard, experiments are being now conducted in our group for the electrochemical characterization of poly-AN/DMA based ionogels.[30,31]

H. D. F. de Melo performed polymer synthesis, swelling experiments, writing of the manuscript, and, with the help of F. Hallwass, acquisition and analysis of NMR experiments, D. S. Carvalho contributed to gel preparation. U. Sternberg performed MDOC simulations and helped in the writing of the manuscript. A. Navarro-Vázquez supervised the project and contributed to the writing and main revision of the manuscript.

The authors thanks Brazilian National Council for Scientific and Technological Development, CNPQ, for financial support (426216/2018-0, and 311683/2019-3) as well as Centro de Tecnologias Estratégicas do Nordeste (CETENE) for computer time with the support of Fundação de Amparo à Ciência e Tecnologia do Estado de Pernambuco (FACEPE) through grant APQ-1864-1.06/12. H. D. F. de Melo and D. S. Carvalho thank CAPES and FACEPE for fellowships IBPG-0611-3.03/19 and IBPG-0485-3.03/19. We thank Prof. B. Luy and Prof. A.C-Pöppler for PDMS and polystyrene gel samples respectively.

Conflicts of interest

A. Navarro-Vázquez is the author of the MSpin program for which he may receive royalties.

Notes and references

‡ Note that all $^{3}J_{HH}$ couplings, including those from Hγ to the methyl group, were explicitly included in the simulation to give a total of fifteen entries.

1 Y. Liu, A. Navarro-Vázquez, R. R. Gil, C. Griesinger, G. E. Martin and R. T. Williamson, *Nat. Protoc.*, 2019, **14**, 217–247.
2 B. Luy, K. Kobzar and H. Kessler, *Angew. Chem., Int. Ed.*, 2004, **43**, 1092–1094.
3 P. Haberz, J. Farjon and C. Griesinger, *Angew. Chem., Int. Ed.*, 2005, **44**, 427–429.
4 R. R. Gil, C. Gayathri, N. V. Tsarevsky and K. Matyjaszewski, *J. Org. Chem.*, 2008, **73**, 840–848.
5 C. Gayathri, N. V. Tsarevsky and R. R. Gil, *Chem. – Eur. J.*, 2010, **16**, 3622–3626.
6 M. E. García, S. R. Woodruff, E. Hellemann, N. V. Tsarevsky and R. R. Gil, *Magn. Reson. Chem.*, 2017, **55**, 206–209.
7 L. F. Gil-Silva, R. Santamaría-Fernández, A. Navarro-Vázquez and R. R. Gil, *Chem. – Eur. J.*, 2016, **22**, 472–476.
8 D. S. Carvalho, D. G. B. da Silva, F. Hallwass and A. Navarro-Vázquez, *J. Magn. Reson.*, 2019, **302**, 21–27.
9 K. A. Farley, M. R. M. Koos, Y. Che, R. Horst, C. Limberakis, J. Bellenger, R. Lira, L. F. Gil-Silva and R. R. Gil, *Angew. Chem.*, 2021, **133**, 26518–26523.
10 D. S. Carvalho, D. G. B. da Silva, F. Hallwass and A. Navarro-Vázquez, *ChemPlusChem*, 2023, **88**, e202200446.
11 H. Weingärtner, *Curr. Opin. Colloid Interface Sci.*, 2013, **18**, 183–189.
12 R. Nanda and K. Damodaran, *Magn. Reson. Chem.*, 2018, **56**, 62–72.
13 K. Damodaran, *Prog. Nucl. Magn. Reson. Spectrosc.*, 2022, **129**, 1–27.
14 A. Mele, C. D. Tran and S. H. De Paoli Lacerda, *Angew. Chem., Int. Ed.*, 2003, **42**, 4364–4366.
15 M. C. Corvo, J. Sardinha, S. C. Menezes, S. Einloft, M. Seferin, J. Dupont, T. Casimiro and E. J. Cabrita, *Angew. Chem., Int. Ed.*, 2013, **52**, 13024–13027.
16 M. Dama and S. Berger, *Carbohydr. Res.*, 2013, **377**, 44–47.
17 J. C. Freudenberger, P. Spiteller, R. Bauer, H. Kessler and B. Luy, *J. Am. Chem. Soc.*, 2004, **126**, 14690–14691.
18 A.-C. Pöppler, H. Keil, D. Stalke and M. John, *Angew. Chem., Int. Ed.*, 2012, **51**, 7843–7846.
19 V. V. Klochkov, R. F. Baikeev, V. D. Skirda, A. V. Klochkov, F. R. Muhamadiev, I. Baskyr and S. Berger, *Magn. Reson. Chem.*, 2009, **47**, 57–62.
20 K. E. Gilbert, GMMX (version 3) **www.serenasoft.com** 2022.
21 T. A. Halgren, *J. Comput. Chem.*, 1996, **17**, 490–519.
22 Y. Zhao and D. G. Truhlar, *Theor. Chem. Acc.*, 2008, **120**, 215–241.
23 R. Holomb, A. Martinelli, I. Albinsson, J. C. Lassègues, P. Johansson and P. Jacobsson, *J. Raman Spectrosc.*, 2008, **39**, 793–805.
24 A. Navarro-Vázquez, *Magn. Reson. Chem.*, 2012, **50**, S73–S79.
25 G. Cornilescu, J. L. Marquardt, M. Ottiger and A. Bax, *J. Am. Chem. Soc.*, 1998, **120**, 6836–6837.
26 C. M. Thiele, V. Schmidts, B. Böttcher, I. Louzao, R. Berger, A. Maliniak and B. Stevensson, *Angew. Chem., Int. Ed.*, 2009, **48**, 6708–6712.
27 P. Tzvetkova, U. Sternberg, T. Gloge, A. Navarro-Vázquez and B. Luy, *Chem. Sci.*, 2019, **10**, 8774–8791.
28 U. Sternberg and R. Witter, *Molecules*, 2022, **27**, 7987.
29 K. Stott, J. Keeler, Q. N. Van and A. J. Shaka, *J. Magn. Reson.*, 1997, **125**, 302–324.
30 M. Wang, P. Zhang, M. Shamsi, J. L. Thelen, W. Qian, V. K. Truong, J. Ma, J. Hu and M. D. Dickey, *Nat. Mater.*, 2022, **21**, 359–365.
31 T. Carvalho, V. Augusto, Â. Rocha, N. M. T. Lourenço, N. T. Correia, S. Barreiros, P. Vidinha, E. J. Cabrita and M. Dionísio, *J. Phys. Chem. B*, 2014, **118**, 9445–9459.